TiO_2 and Al_2O_3 ultra thin nanolaminates growth by ALD; instrument automation and films characterization

H. Tiznado*, D. Domínguez, W. de la Cruz, R. Machorro, M. Curiel and G. Soto
Universidad Nacional Autónoma de México, Centro de Nanociencias y Nanotecnología, Km. 107 Carretera Tijuana-Ensenada, Ensenada, 22860, Baja California, Mexico.
** CNyN-UNAM, P.O. Box 439036, San Ysidro, CA, 92143-9036, USA.*
Tel: +52+646+1744602, Fax: +52+646+1744603

Recibido el 28 de octubre de 2011; aceptado el 30 de agosto de 2012

We report on the development of a fully operational atomic layer deposition (ALD) system. This system is computer-controlled and can deposit multilayered systems without user intervention. We describe the design of manifold, reaction chamber and exhaust. Additionally we give some features of the automatization software and electronics. To evaluate the ALD performance we used as precursor trymethyl aluminum (TMA) and tetrakis (dimethylamino) titanium (TDMAT) to deposit Al_2O_3 and TiO_2, respectively, in nanolaminated film structures. The thicknesses and composition of the films are precisely controlled, as determined by spectroscopic ellipsometry, and the nanolaminates have a sharp interface as indicated by Auger depth profile.

Keywords: Atomic layer deposition; nanolaminates; instrumentation; automation; ellipsometry.

PACS: 07.30.Kf; 77.84.Bw

1. Introduction

Atomic layer deposition (ALD) is a powerful thin film deposition technique. Currently it is important in a wide range of applications. In semiconductor industry it is used to process gate dielectrics, gate electrodes, metal interconnects, diffusion barriers and capacitors. For optical applications, it is used to produce optical filters, transparent conductors, solar cells, antireflection coatings and photonic crystals. Also it is important for the manufacturing of fuel cells, catalyst, anticorrosion and biocompatible materials. The list can continue with prospective applications of emerging areas of nanotechnology [1]. Due to the extraordinary capability provided by the ALD technique for producing films with controlled stoichiometry and thickness at the atomic scale, we decided to develop an ALD capability in our laboratory. Our main requirement is the instrument to be competitive with commercial systems at lower costs. The objective in this work is to present our implementation of an automated ALD system capable of depositing several layers of different materials and capable to be upgraded for integration of in situ characterization techniques *e.g.* ellipsometry or infrared spectroscopy. We also present our considerations for the manifold, reaction chamber and exhaust design, as well as the control electronics and software. To test and calibrate the system, films of Al_2O_3, TiO_2, and nanolaminates TiO_2-Al_2O_3 were grown and characterized. We chose as example this structure because of its importance for the microelectronic industry [2].

2. ALD basics

ALD can be classified within the Chemical Vapor Deposition (CVD) methods, where its fundamental variant is the repetitive self-limiting surface reactions to control the growth of films, typically producing a maximum of one atomic layer at a time [1]. The ALD materials are assembled bottom up, layer-by-layer, where ideally a single element composes the discrete layer. The typical ALD process is well represented by the ALD growth of Al_2O_3. The Fig. 1 shows a scheme for one ALD cycle. The process can be divided in two-half reactions. The first one is the self-limited chemical adsorption of trimethyl aluminum (TMA_{ad}), Fig. 1(a). The sample is exposed to TMA long enough to saturate the surface. Then, the excess of TMA, which is in the gas phase ($TMA_{(g)}$), is purged out by an inert gas flow, Fig. 1(b). In the second-half reaction, Fig. 1(c), the $TMA_{(ad)}$ is exposed to water vapor in order to oxidize it to Al_2O_3. Again, the water exposition

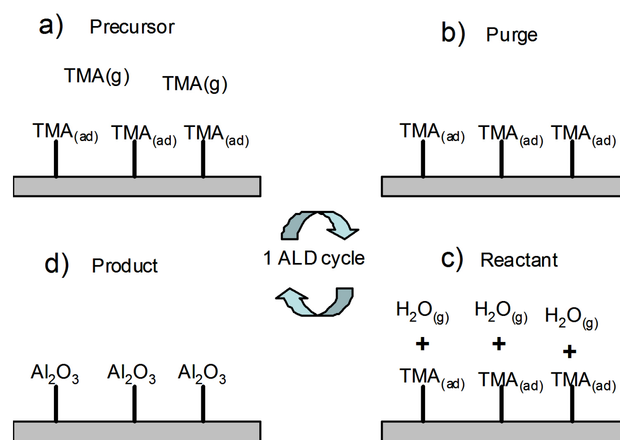

FIGURE 1. Schematic representation of the surface reactions required for the growth of an Al_2O_3layer. (a) TMA condense in the substrate surface, (b) surplus TMA is purged out from the reaction chamber, (c) H_2O is admitted and it reacts with the adsorbed TMA, (d) water is flushed out from the system. The product of one ALD cycle is about a monolayer of Al_2O_3.

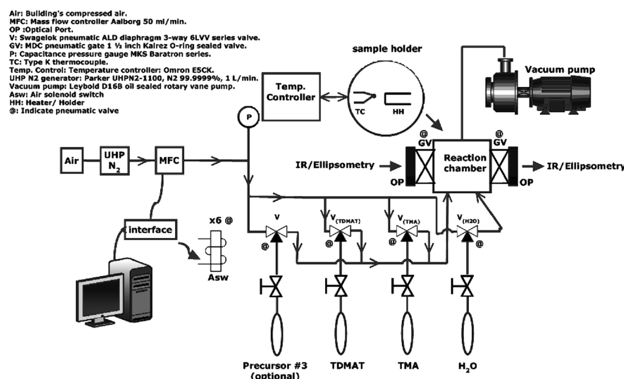

FIGURE 2. Scheme of the warm-walls ALD system.

should be enough to completely oxidize all the $TMA_{(ad)}$ molecules. Finally, the excess of water (gas phase) is purged out, Fig. 1(d). These two half-reactions completes one ALD cycle, which results in certain thickness of Al_2O_3. The above reactions, particularly the first-half, should be done within a temperature range on the substrate surface; the high limit is set by the decomposition of the TMA precursor and the low limit is set by its condensation on the surface. The suitability of the ALD precursors is very crucial. They need to have appropriate chemical and physical properties, namely, they must be thermally stable and sufficiently volatile for easy transport. Also, the two reactants involved must exhibit the appropriate chemistry. That is, their surface conversion must be fast, complete, irreversible, self-limiting and must occur at suitable low temperatures. Additionally, the reactions need to be complementary, in specific, each needs to be able to prepare the surface for the other and to lead to the formation of oxides with the right stoichiometry .

There are several advantages to the use of ALD over other film deposition methods like chemical (CVD) or physical vapor deposition (PVD). Among them: (1) the film thicknesses depend only on the number of cycles employed, not on the exposures used in each cycle, so the control of film thickness is simplified and more accurate; (2) the reactant flux homogeneity in the deposition reactor is not as strict as in CVD, so the processes are more reproducible and easy to scale up for large-area coatings without sacrificing conformality; (3) in terms of temperature and reactant flows, there is more flexibility in the design of the operational conditions for the deposition; (4) interferences from gas-phase reactions are often avoided because of the separation of the two half-reactions in time, (5) ALD is the best technique to grow atomically uniform layers on high aspect ratio 3-D structures. On the negative side, ALD suffers from some intrinsic limitations, including (1) the deposition of undesirable contaminants within the growing films because of the decomposition of the precursors via side reactions, (2) the growth of films with different microstructures and morphologies from those obtained by PVD, and (3) the time periods of the deposition could be long if the ALD system is not optimized, since only a fraction of a monolayer is deposited per cycle [4].

3. The ALD system

Our ALD setup is a low-volume closed system designed to transport the precursors and carrier gas efficiently from the manifold to the substrate, and then to the exhaust. Figure 2 is a scheme of the warm-walls ALD system. It is purposely built for the consecutive deposition of Al_2O_3 and TiO_2, although it can be used with other precursors to deposit different materials. It consists of manifolds, deposition chamber and exhaust, all stainless steel. Two independent manifolds were implemented: The first one with ampoules of trymethyl aluminum (TMA) and tetrakis (dimethylamino) titanium (TDMAT); the second one is used to separately supplement water as oxidizing agent. The second manifold is convenient to prevent the oxide build up on the main manifold walls, leading eventually to poor purging rates. The oxide growth is a consequence of the chemically adsorbed precursor (after each pulse) on the manifold walls, and it cannot be avoided even if the gas phase of the chemical precursors is completely purged out of the system. Thus, if the water source is placed in the same manifold, oxide deposits grows at a higher rate. Using our setup, the backflow of water into the precursors manifold can be kept at minimum by the carrier gas flow. The key components in the manifolds are the 3-way valves which help to minimize the dead volume. The valves work in two modes: purge or pulse. In the purge mode, the carrier gas (N_2 in our case) flows through the permanently open valve ports, constantly purging the entire manifold. In the pulse mode, the normally closed port is opened for a short time (typically tens of milliseconds), allowing the vapor phase of the chemical precursor or water to enter into the carrier gas stream. The deposition chamber is fitted with two optical transparent ports, which are kept contamination-free from reactants by isolating the ports with gate valves. These ports can be used to upgrade the system with *in situ* optical spectroscopies, like infrared or transmittance ellipsometry.

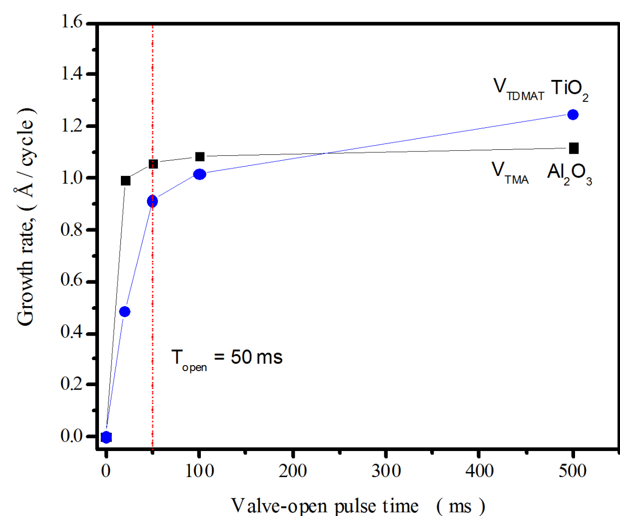

FIGURE 3. Al_2O_3 and TiO_2film thickness as a function of their respective precursor pulse time (valve-open).

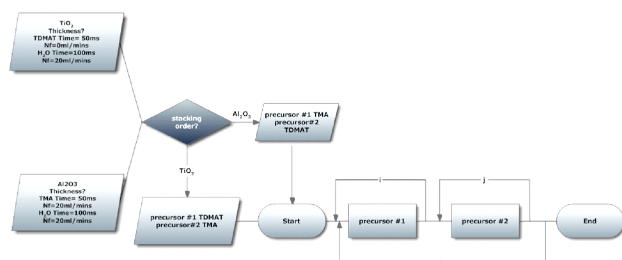

FIGURE 4. Flow chart of the LabView program for depositing stacked TiO_2/Al_2O_3 nanolaminates. The "i" and "j" are the number of cycles for each oxide (specific thickness). The "k" is the number of stacks (overall thickness).

The solid substrate *e.g.*, silicon or glass samples of about 1 cm^2, is resistively heated by a square "U" shaped stainless steel sheet heater. The configuration of the sample holder/heater allows positioning the sample in the optical ports line of view. A variable transformer, temperature controller and thermocouple spring fastened on top of the sample keep the preselected temperature of the sample. To help pumping out rapidly the residual gasses, the exhaust is keep as straight as possible, with 3/4 tubing; it is larger than the manifold tubing, 1/4 inch. The whole system, including the exhaust, is wrapped with heating tape and warmed up to about 80°C to avoid condensation of the precursors on the walls.

4. Automation of the ALD system

As previously mentioned, the ALD system was built for the deposition of thin film oxides. In this work we prepared films based on Al_2O_3 and TiO_2. The Al precursor was trymethyl aluminum (TMA) with a vapor pressure of ~8.7 Torr at room temperature. The Ti precursor was tetrakis (dimethylamino) titanium (TDMAT) with a vapor pressure of ~1.1 Torr at 60°C. The whole ALD system was heated at 80°C and the sample at 100°C. N_2 carrier flow was set at 20 ml/min. Al_2O_3 and TiO_2 films were deposited on silicon (111) substrates at 100°C. Under these conditions, the measured pressure at the manifold and exhaust (pressure gauge at the pump entrance) was ~1.5 and ~0.12 Torr, respectively. The system needs to be pre-calibrated in the current conditions to find the adequate open-valve pulse time of reactive; this is done manually by the user. In order to determine this crucial time for TMA and TDMAT, 20 cycles of Al_2O_3 or TiO_2 precursors were delivered with different pulse times for each precursor. The thickness was determined by spectroscopic ellipsometry. Figure 3 shows the Al_2O_3 and TiO_2 thin film growth rate as a function of the TMA and TDMAT precursor pulse time. Good saturation of the growth rate is observed for Al_2O_3 at a pulse time of 50 ms of the TMA precursors. For this pulse time, the Al_2O_3 film grows at 1.1 Å/cycle. As a comparison, the Al_2O_3 film growing rate at 100°C has been reported at 0.93 Å/cycle for TMA and O_3 [5], which is consistent with our result. However, it is reported up to 1.7 Å/cycle for TMA and N_2O plasma [6] at the same growing temperature. In contrast to the Al_2O_3 film, the growth rate of TiO_2 film did not saturate with increasing the TDMAT exposure time, although a clear decreasing of the growth rate is observed at 50 ms pulse time. This result indicates the self-saturation of the TDMAT is not perfect, probably due to some decomposition of the TDMAT, despite its decomposition temperature is reported at 180°C [7]. A similar result has been reported in Ref 8. Good self-saturation has been reported at 50°C [9]. The growth rate for our TiO_2 samples at 50 ms pulse time is 0.9 Å/cycle, which agrees well with other report [9]. From the calibration procedure we chose 50 ms for both, TMA and TDMAT, as a safe valve-open time width; with this value we keep away from TDMAT goes into in CVD-mode.

The automation consists of a LabView™ computer program and complementary interface electronics to control the pneumatic valves and MFC. The interface electronics is used to electrically isolate the parallel computer port. It also works as the power and logic stages to toggle the status OPEN/CLOSED of the valves and the LOCAL/REMOTE control of the mass flow controller, MFC. The computer program requires two kinds of input parameters: user input and semi-fixed. The user input parameters are the stack layer-order, the number of ALD cycles for each layer (***i***, ***j***) and the number of stacks (***k***). From the previous calibration, the purge flow and purge time, the temperature of walls, the sample temperature, the valve-open pulse width for each precursor (T_{TMA}, T_{TDMAT}) are written in the semi-fixed parameters register. If new preparation conditions are needed, for instance a different deposition temperature, a new pre-calibration is obligatory, and the new set of parameters should be recorded in the semi-fixed parameter-register. The flow chart of deposition is shown in the Fig. 4. The program after receiving the input parameters, nests several sequences in which automatically makes the deposits.

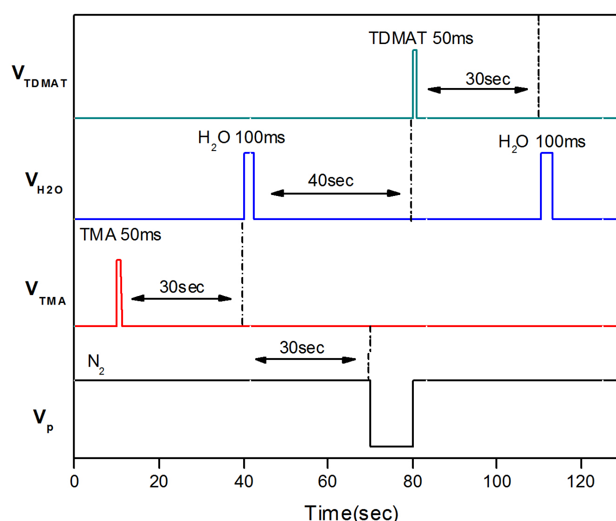

FIGURE 5. Timing diagram of control signal to manifold valves to deposit a layer of TiO_2 on top of Al_2O_3. Valve open is high, low is closed. Times of pulses are not to scale.

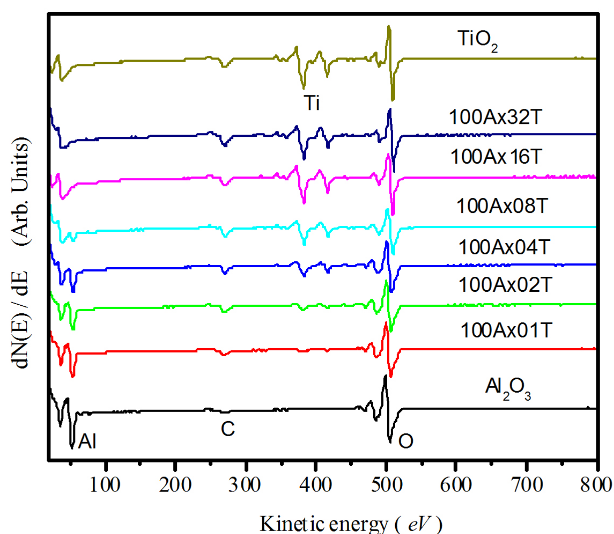

FIGURE 6. Determination of the TiO_2 overlayer by AES with an increasing number of TDMAT-H_2O cycles. This overlayer is grown on top of Al_2O_3 film, which is obtained after 100 cycles of TMA-H_2O (equivalent to 114 Å).

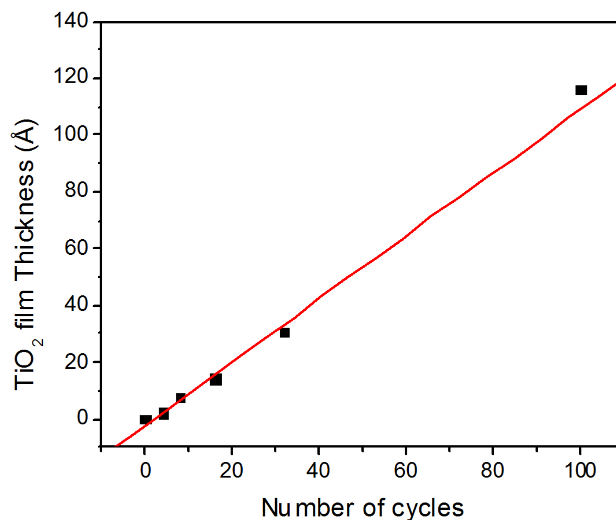

FIGURE 7. Thickness of a TiO_2 overlayer with an increasing number of TDMAT-H_2O cycles, as determined by ellipsometry. This overlayer is grown on top of Al_2O_3, which is obtained after 100 cycles of TMA-H_2O (equivalent to 114 Å).

The Fig. 5 shows a representative timing diagram to deposit one ALD cycle of Al_2O_3, followed by one cycle of TiO_2. The normal state of the manifold is the N_2 flowing throughout the entire system: purging mode (PM). It was determined that 30 seconds in the PM is more than enough to purge out the gas phase of the both precursors and water. The sequence starts in the PM, then, the valve for the TMA precursor, V_{TMA}, opens for a preselected time (pulse) sufficient to saturate the substrate surface with chemically adsorbed TMA. Immediately after, the system goes back to PM for 30 seconds, and a water pulse, V_{H_2O}, is activated. The water pulse time should be enough to oxidize the previously adsorbed TMA to Al_2O_3. The manifold then goes to PM, completing the first ALD cycle. Next, to be able to dose the TDMAT, which is previously heated up to 60°C to raise its vapor pressure above 1 Torr, the N_2 flow is stopped for 10 seconds to lower the manifold pressure from about 1.5 to 0.1 Torr. The advantage of lowering the manifold pressure for low vapor pressure precursors is that the use of a bubbler is avoided. At this point, the TDMAT pulse, V_{TDMAT}, is dosed. After its respective PM time, the water pulse oxidizes the adsorbed TDMAT. Then, the manifold goes back to PM to purge the water excess, closing the ALD cycle for TiO_2.

5. Instrument Validation

Figure 6 shows a series of Auger electron spectroscopy (AES) for samples grown on a Si substrate with a TiO_2 overlayer on top of an Al_2O_3 layer of 100 cycles. The thickness of the overlayer is built up with 0, 1, 2, 4, 8, 16 and 32 TiO_2 cycles. The samples are labeled as 100Ax*T, where * is the number of TiO_2 cycles. For comparison, a TiO2 film was prepared using 120 growth cycles. The spectrum for the 100Ax0T sample (Al_2O_3 thickness: 114 Å) shows peaks for Al, O and C. The presence of C indicates incomplete oxidation of the TMA due to the low temperature of the process. Next, the Auger peak for Ti is already seen for the 100Ax1T sample, and then, as the number of TiO_2 cycles is increased, the intensity for the Ti peak goes up at expenses of the Al peak intensity. For the 100Ax32T sample, the Al peak is barely detected in its corresponding spectrum, which is very similar to that of the only TiO_2 sample. This result indicates that the TiO_2 overlayer is covering up the Al_2O_3 film in a controlled manner. The corresponding TiO_2 thickness measured by ellipsometry is indicated in the Fig. 7. It is seen a nearly linear growth of the TiO_2 on top of the Al_2O_3 film, which agrees well with the trend observed in AES.

Figure 8 shows the Ar^+ sputter AES depth profile for a 100Ax100T sample grown on a Si substrate. The erosion was

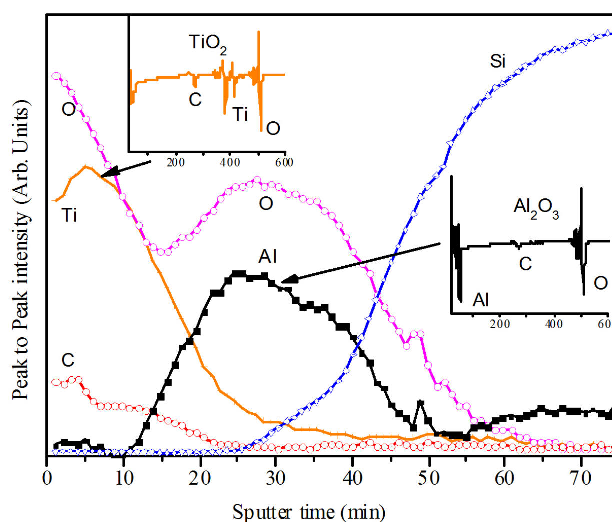

FIGURE 8. Auger depth profile for a TiO_2/Al_2O_3 /SiO_2 (native)/Si layered system.

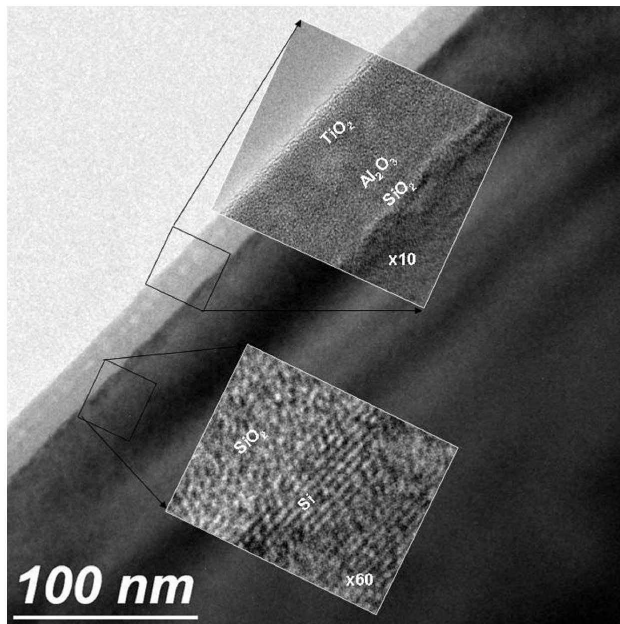

FIGURE 9. Cross section TEM image of the ALD nanolaminate 100Ax32T.

set at a slow rate to be able to detect the details of the Al_2O_3-TiO_2 interface. Three different zones are easily distinguishable as a function of sputter time. The first zone, which is the material close to the surface, is composed of Ti, O and C. The insert shows that this corresponds to TiO_2 with an evident amount of residual C. In the second zone we found Al and O, with traces of C, as shown in the second insert. The Third zone is composed of Si. The evolution of the Ar^+ depth profile needs some clarification. Initially, the Ti intensity increases due to the removal of adventitious C. However, the O signal decreases, which could indicate that some oxygen is removed simultaneously with carbon in C-O or O-C-O bonds. The surface appears to be C and O rich, while the volume is Ti-rich. However it might be an artifice of the Ar^+ sputtering since it shows preferential erosion for the lighter atoms, C and O in this case. As the interfacial zone is reach, the Ti signal goes down and the C signals continue to decrease, while the both Al and O signal start to increase. Finally, as the Al and O signals start to go down, the Si signal from the substrate increases. It is observed that the traces for depletion of Ti and the simultaneous emergence of Al are both nearly a lineal rate, which suggests that the Ti-Al interface is sharp, as expected for ALD films. From the depth profile result is evident that the system still needs a fine-tuning to remove the unwanted carbon contamination, specifically in the deposition of TiO_2, which appears to be chemically enlaced to the material via C-O bonds.

In Fig. 9 is shown a low magnification cross-section TEM image for the 100Ax32T sample. The dark gray area must be the silicon substrate, while the light gray zone is the top layer consisting of TiO_2, Al_2O_3 and the SiO_2 native oxide, in agreement with the previous Ar^+ sputter AES depth profile. In higher-magnifications, A-inset of Fig. 9, is possible to observe the interplanar spacing of the silicon substrate. The TEM analysis provided evidence that the top layer consists of amorphous material. The B-inset shows the interfaces to the substrate. Observe the light tone of gray that is ascribed to the native SiO_2 layer typical of the silicon ($\sim$2 nm). A slight variation in tone suggests the presence of a dissimilar density material that is due to the aluminum oxide layer growth by ALD on top of the native SiO_2. In the B-inset is observed a continuous tone of gray that corresponds to the ALD Al_2O_3 and TiO_2 bilayer. Due to the amorphous nature of the processed materials the interface between those two materials

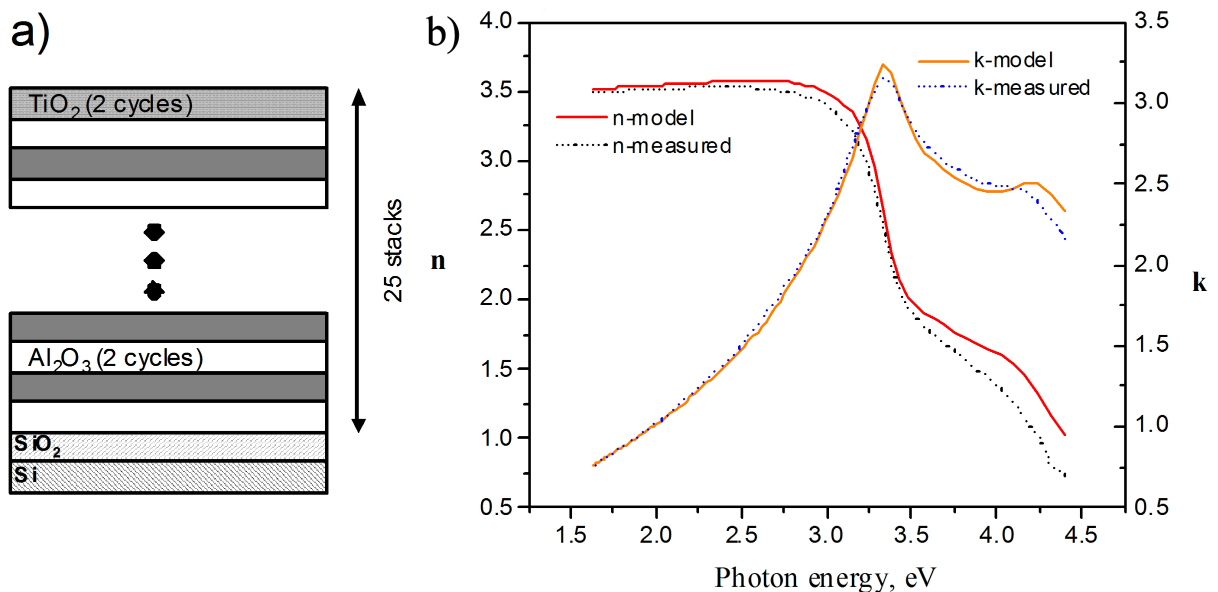

FIGURE 10. a) Scheme of the 25 stacks structure, each stack consisting of 2 Al_2O_3 cycles, followed by 2 TiO_2 cycles and, b) measured and model refraction index, n, and extinction coefficient, k, obtained by means of spectroscopic ellipsometry.

could not be easily distinguished, except by some irregularities at the interface. It is therefore difficult to determine the exact thickness of each individual layer by TEM. The overall thickness of the ALD bilayer could be roughly estimated at about 15 nm, which is relatively close with the growth rates estimated with ellipsometry, as we will discus in the next section.

6. Nanolaminated structures

Multilayer coatings of alternatively ordered thin films of transition metal oxides with nanoscale thickness are known to have properties superior than that of a single film. The decisive role has been assigned to the variety of singularities occurring at the interfacial region of the thin composing films. Recently it was reported high-k AlO_x-TiO_y nanolaminated structures, which position them as a good candidate for replacing the SiO_2 gate dielectric [2]. We decided to test the ALD system building a structure of ultra-low thickness layers, comparable to those produced by Li et al. We prepared a 25 stacks structure, with each stack consisting of two Al_2O_3 cycles, followed by two TiO_2 cycles. The Fig. 10a shows a scheme of the grown structure. The film was prepared according to the experimental parameters found in the calibration. The refractive index n and the extinction coefficient k of the TiO_2/Al_2O_3 nanolaminates were measured, using spectroscopic ellipsometry with different incident light energies, to verify that the expected heterostructure was achieved, Fig. 10b. A model of 25 Al_2O_3/TiO_2 layers was used to fit the experimental data. The fitting yielded 2.5 and 2.0 Å thickness for the Al_2O3 and TiO_2 layers, respectively. This result is reasonably close to the corresponding growth rates obtained in the calibration experiment (1.1 and 0.9 Å/cycle for Al_2O_3 and TiO_2 films, respectively). With this result, the total thickness adds up to $\sim$112 Å, which is close to the expected 100 Å calculated with the calibration growth rates. The difference could be a result that the optical constants used for the model could not be accurate enough for ultra thin oxides. From a dielectric point of view the interface is neither Al_2O_3 nor TiO_2. This implies that the optical response of the overall system should change since it is affected many times by this transitional region. This seems to agree with the work of Li *et al.* [1], which shows that the dielectric function of AlO_x-TiO_y nanolamintes, measured at 10^2-10^6 Hz, changes as the oxide layer thickness goes below 1 nm. They conclude that AlO_x-TiO_y interface works as a charge trapping region (a capacitor). Although in our case the ellipsometric measurements are obtained in a different region of the electromagnetic spectrum, it is possible that the optical constants have varied since our thicknesses approximate to the limit where the charging trapping effect is reported to occur. Further work with REELS (reflection electron energy loss spectroscopy) and ellipsometry measurements is being done to investigate the behavior of the optical properties at different energies. Nevertheless, we conclude that the applied model is suitable, and that the control of the growth rate is excellent for the build of nanolaminated structures.

7. Conclusion

We have designed and constructed a fully automated ALD system. The system is capable of depositing TiO_2/Al_2O_3 nanolaminates, without user intervention, in a controlled manner and with sharp interfaces. Since ALD accumulate one atomic layer in each cycle, stacked multi-component system can be deposited with complete control at the nanometre scale by changing the reactants in sequential order. This was demonstrated in the present application, where the Al_2O_3 film growth (from TMA precursor) showed a nearly ideal ALD behavior, while the TiO_2 film (from TDMAT) had a somewhat CVD behavior. Nevertheless, the thickness was well controlled under the experimental conditions used. The chemical composition of the films showed some carbon contamination, which can be avoided at higher processing temperatures. Ultra-thin films of a few nanometres can be deposited in a precisely controlled way by our system, making it a true technological device to build nanostructures.

Appendix I

Film characterizations

The chemical composition and depth profile of the films was determined by Auger electron spectroscopy in a PHI-548 instrument. Ellipsometric measurements were carried ex situ with a multi-wavelength rotating analyzer instrument, M-44, made by J.A. Woollam Co., covering the 1.625 to 4.405 eV photon-energy range. Data analysis was performed with the software WVASE32^{TM} [10]. Thickness of films was obtained indirectly using an iterative least-squares minimization. The process is started by considering the optical constants of Al_2O_3 and TiO_2 (refractive index and extinction coefficient) from references [11]. An approximation of thickness for all individual layers of sample, including the correct layer sequence, together with the native SiO_2 oxide layer, $\sim$20 to 30 Å, all over an infinite silicon substrate, are used as input to the numerical model. The unknown thickness parameters were varied, and the ellipsometric angles (Ψ and Δ) are calculated using the Fresnel equations. The calculated n and k values which best match the experimental data provide the thickness parameters of the sample. The consistence between different samples gives confidence to this procedure [11].

Acknowledgments

This work was financially supported by CONACyT grants #83275 and #82984, and DGAPA IN114209-3. We acknowledge the technical assistance of A. Tiznado, E. Medina, J. Díaz and P. Pizá.

1. H.S. Nalwa, *Handbook of Thin Films Materials, Deposition and Processing of Thin Films* Vol. 1 (Academic Press 2002). pp. 103.
2. W. Li, Z. Chen, R.N. Premnath, B. Kabius, and O. Auciello *Journal of Applied Physics* **110** (2011) 024106-1 – 024106-8.
3. M. Leskela, M. Ritala, ALD precursor chemistry: Evolution and future challenges, *Journal De Physique IV* **9** (1999) 837-852.
4. H. Tiznado and F. Zaera, *Journal of Physical Chemistry B* **110** (2006) 13491-13498.
5. S.K. Kim, S.W. Lee, C.S. Hwang, Y.S. Min, J.Y. Won, J. Jeong, *Journal of the Electrochemical Society* **153** (2006) F69-F76.
6. S. Lee, H. Jeon, *Electronic Materials Letters* **3** (2007) 17-21.
7. J.W. Elam, M. Schuisky, J.D. Ferguson, and S.M. George, *Thin Solid Films* **436** (2003) 145-156.
8. W.J. Maeng and H. Kim, *Electrochemical and Solid State Letters* **9** (2006) G191-G194.
9. Q. Xie *et al*., *Journal of Applied Physics* **102** (2007) 083521-1 – 083521-6.
10. J.A. Woollam Co., (Guide to Using WVASE32^{TM}, Inc., 1997).
11. E. D. Palik, *Handbook of Optical Constants of Solids* (Academic Press, Boston, 1985).
12. R. M. A. Azzam and N. M. Bashara, *Ellipsometry and Polarized Light* (North-Holland, Amsterdam, 1987).